Supporting Information

Wiszniak et al. 10.1073/pnas.1419368112

SI Experimental Procedures

Histology and Immunolabeling. Embryos were fixed in 4% (wt/vol) formaldehyde in PBS. Cryosections were stained with Von Kossa (1% silver nitrate) to mark areas of mineralization, and Alcian blue (0.1% Alcian blue in 0.1M HCl) to mark cartilage and counterstained with eosin. For immunolabeling, cryosections, whole-mount embryos, or aortic rings were blocked in 10% (vol/vol) protein block, serum-free (DAKO), 0.2% BSA, 0.2% Triton X-100 in PBS, and stained with the indicated primary antibodies. Antibodies used were rabbit anti-Sox9 (Millipore) 1:1,000, rabbit anti-p75 (Epitomics) 1:200, rabbit anti-phospho-histone H3 (PHH3) (Millipore) 1:500, rabbit anti-cleaved-Caspase-3 (Cell Signaling Technology), rat anti-CD31 (Biolegend) 1:150, goat anti-Nrp1 (R&D) 1:200, rat anti-Endomucin (Santa Cruz) 1:50, mouse anti-alpha smooth muscle actin (Sigma) 1:2,000, mouse anti-Tuj (Sigma) 1:750, chicken anti-GFP/YFP (Millipore) 1:1,000, goat anti-collagen IV (Millipore) 1:300, and biotin conjugated Isolectin B4 (Sigma) 1:1,000. TUNEL staining was performed following the manufacturers recommendations (Roche *In Situ* Cell Death Detection Kit, TMR Red). Cryosections were mounted in Prolong Gold antifade reagent with DAPI (Molecular Probes). Confocal images were acquired on a LSM 700 (Zeiss) system.

Skeletal Preparations. Alcian blue and Alizarin red staining of cartilage and bone was performed as described (1).

In Situ Hybridization. Section in situ hybridization was performed as described (2). Riboprobes were transcribed from plasmids containing the cDNA sequences for *Vegfa 164*, *Sox10*, *Msx1*, *Dlx5*, or *Col2a1*.

β-Galactosidase Staining. Cryosections were incubated in staining solution: 19 mM sodium dihydrogen phosphate, 81 mM disodium hydrogen phosphate, 2 mM $MgCl_2$, 5 mM EGTA, 0.01% sodium deoxycholate, 0.02% Nonidet P-40, 5 mM potassium ferricyanide, 5 mM potassium ferrocyanide, and 1 mg/mL X-gal substrate at 37 °C until blue staining was clearly visible.

Primary NCC and Aortic Ring Culture. NCCs and aortic rings were grown as previously described (1, 3). Aortic rings were embedded in collagen and plated onto 35-mm culture dishes (IBIDI), or directly on top of primary NCCs that had been cultured for 24 h. Vessel sprouting was induced by addition of 20 ng/mL rhVEGF165 (R&D Systems), and VEGF function was inhibited by addition of 180 ng/mL sFlt1 (R&D Systems). Tissues were cultured for 6 d and fixed and stained as described earlier.

ATDC5 and Aortic Ring Culture. The murine prechondrogenic cell line ATDC5 (4) was cultured in DMEM/F12 with the addition of 5% (vol/vol) FCS. For coculture experiments, ATDC5 cells were grown to confluence in 24-well plates before addition of aortic rings embedded in collagen directly on top of ATDC5 cells. For conditioned media experiments, aortic rings were embedded in collagen with media collected after 1 d of growth and applied directly to ATDC5 cultures. This was repeated daily for 5 d in total. Cell proliferation was quantitated as the number of PHH3-positive nuclei per square millimeter from nine images from $n = 3$ experiments.

Primary Meckel's Chondrocyte Culture. Primary Meckel's cartilage chondrocytes were isolated using a protocol modified from Ishizeki et al. (5). Briefly, Meckel's cartilage bars were dissected from E14.5 wild-type mouse embryos. Cartilage was digested with 0.15% trypsin (Gibco), 0.1% EDTA in DMEM for 30 min, washed with PBS, and then further digested with 0.15% collagenase type II (Worthington) in DMEM for 30 min, both at 37 °C. Dissociated cells were plated onto 50 μg/mL fibronectin-coated 48-well culture plates at a density of 1×10^5 cells per well. Cells were cultured in DMEM/F12 containing 5% (vol/vol) FCS. After 2 d of initial culture, aorta conditioned media was applied directly to primary chondrocytes, and this was replenished daily for 5 d in total. Cell proliferation was quantitated as the number of PHH3-positive nuclei per square millimeter from 18 images from $n = 3$ experiments, with independent tissue isolations for each experiment.

Analysis of Hemifacial Microsomia Patients. A subset of six patients, all with severe skeletal manifestations of hemifacial microsomia (S3 on skeletal, auricle, and soft tissue classification), had all their radiological investigations reviewed. In all cases, this included an orthopantomogram radiograph, but most had undergone computed tomography scans (with 3D reconstruction) as part of their surgical evaluation. The images were carefully reviewed, with particular attention paid to the entry, then the subsequent intra mandibular course, and finally the exit of the inferior alveolar neurovascular bundles.

Statistical Analysis. All data are presented as mean ± SEM and analyzed using Student's t test. In all studies, a P value of <0.05 was considered to be statistically significant.

1. Wiszniak S, et al. (2013) The ubiquitin ligase Nedd4 regulates craniofacial development by promoting cranial neural crest cell survival and stem-cell like properties. *Dev Biol* 383(2):186–200.
2. Schwarz Q, et al. (2004) Vascular endothelial growth factor controls neuronal migration and cooperates with Sema3A to pattern distinct compartments of the facial nerve. *Genes Dev* 18(22):2822–2834.
3. Baker M, et al. (2012) Use of the mouse aortic ring assay to study angiogenesis. *Nat Protoc* 7(1):89–104.
4. Shukunami C, et al. (1996) Chondrogenic differentiation of clonal mouse embryonic cell line ATDC5 in vitro: Differentiation-dependent gene expression of parathyroid hormone (PTH)/PTH-related peptide receptor. *J Cell Biol* 133(2):457–468.
5. Ishizeki K, Takigawa M, Nawa T, Suzuki F (1996) Mouse Meckel's cartilage chondrocytes evoke bone-like matrix and further transform into osteocyte-like cells in culture. *Anat Rec* 245(1):25–35.

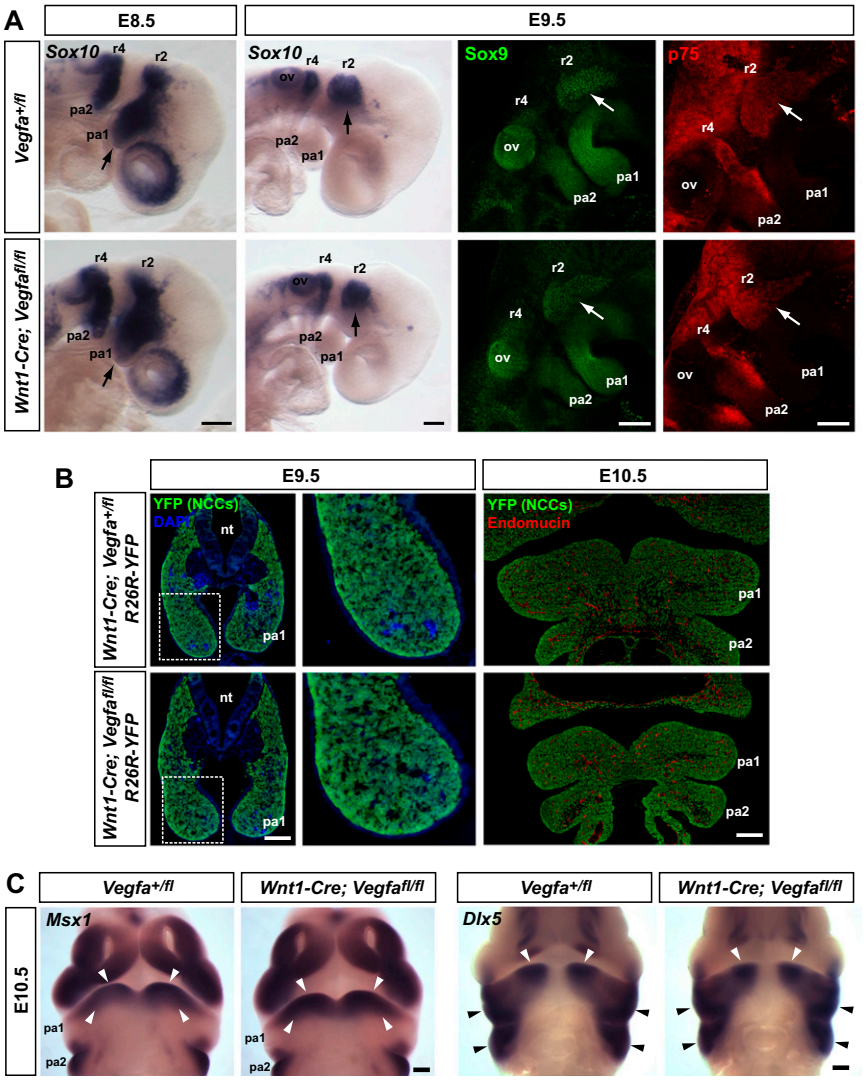

Fig. S1. Early NCC development is normal in *Wnt1-Cre;Vegfa*$^{fl/fl}$ mutant embryos. (*A*) Control (*Upper*) and mutant (*Lower*) E8.5 and E9.5 embryos were stained with markers of early migrating NCCs; *Sox10* in situ hybridization, Sox9 and p75 antibody staining. There did not appear to be any significant differences in staining between control and mutant embryos (arrows). pa, pharyngeal arch; ov, otic vesicle; r, rhombomere. (Scale bar, 200 μm.) (*B*) Control (*Upper*) and mutant (*Lower*) embryos with a R26R-YFP transgene present to lineage trace NCCs and derivatives. (*Left*) Transverse sections through pa1 show lineage tracing of NCCs at E9.5 with no deficiency of NCC migration and population of pa1. (Scale bar, 100 μm.) (*Right*) Frontal sections through pa1 at E10.5 show no loss of NCC density in pa1. Costaining with endomucin demonstrates interaction of NCCs with blood vessels in both control and mutant embryos. nt, neural tube. (Scale bar, 200 μm.) (*C*) In situ hybridization for *Msx1* (*Left*) and *Dlx5* (*Right*) at E10.5 in control and mutant embryos demonstrates specification of pa1 and pa2 mesenchyme occurs normally in *Wnt1-Cre;Vegfa*$^{fl/fl}$ mutants (arrowheads). (Scale bar, 200 μm.)

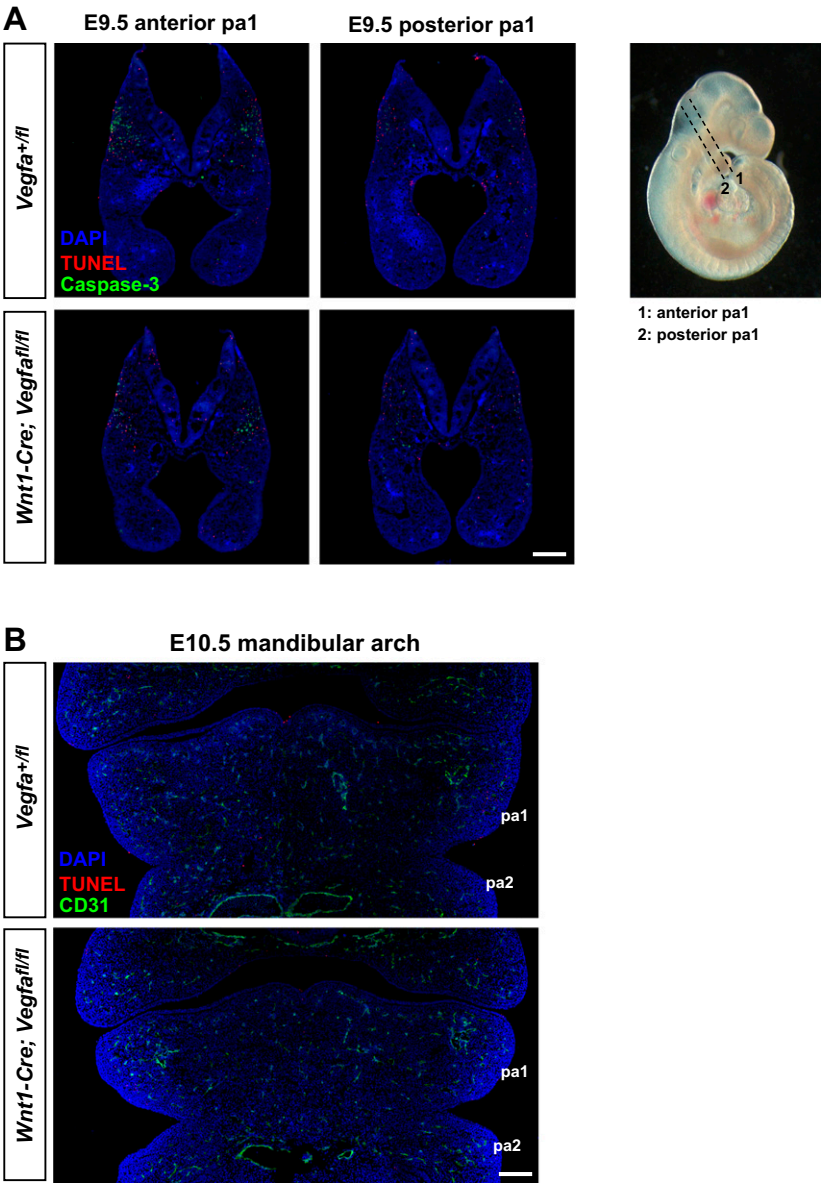

Fig. S2. Analysis of cell death in E9.5 and E10.5 *Wnt1-Cre;Vegfa*$^{fl/fl}$ embryos. (*A*) Transverse sections through pa1 in E9.5 control and *Wnt1-Cre;Vegfa*$^{fl/fl}$ embryos. Anterior (*Left*) and posterior (*Right*) sections are shown, and the plane of section is indicated on the embryo diagram to the right. Sections were immunostained with markers of cell death, TUNEL and cleaved-caspase-3, and counterstained with DAPI. Cell death is evident in both control and mutant embryos, particularly in the anterior pa1; however, no increased cell death was observed in the mutants. (Scale bar, 100 μm.) (*B*) Frontal sections through pa1 in E10.5 control and mutant embryos immunostained with CD31 and TUNEL and counterstained with DAPI. Minimal cell death is evident in pa1 at E10.5, and no differences were observed between control and *Wnt1-Cre;Vegfa*$^{fl/fl}$ embryos. (Scale bar, 200 μm.)

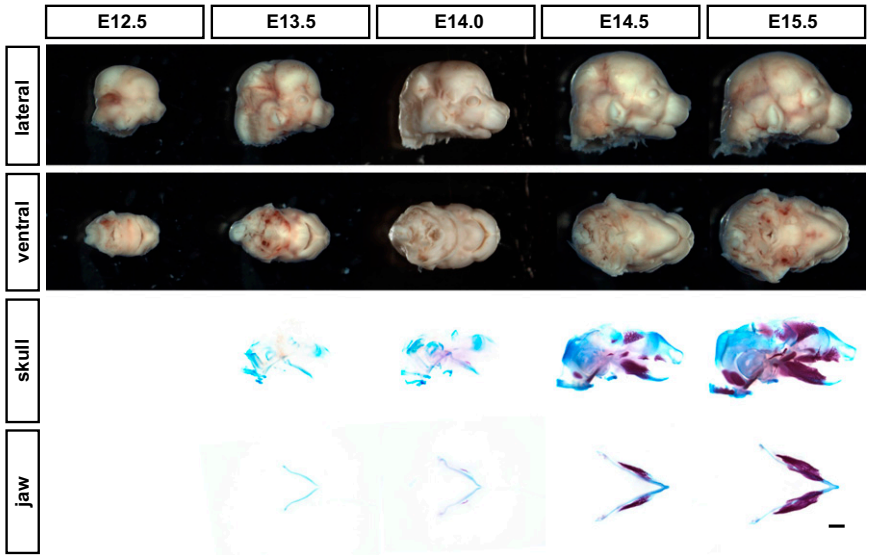

Fig. S3. Jaw development from E12.5 to E15.5. (*Top*) Lateral and ventral views of embryonic heads from wild-type embryos from E12.5 to E15.5. The shape of the jaw changes dramatically between E13.5 and E14.5, as it extends outward toward the tip of the maxilla. After E14.5, the jaw maintains this shape and increases in overall size in proportion with the rest of the head. (*Bottom*) Lateral views and dissected jaws of embryos stained with Alcian blue and Alizarin red to label cartilage and bone, respectively. Bona fide cartilaginous Meckel's cartilage is first evident at E13.5 and exhibits a bowed shape with both cartilage arms concave relative to each other. The tip of Meckel's cartilage also points caudally downward. At E14.0, Meckel's cartilage is bowed and the first evidence of mineralization is visible at the mandibular ossification centers. By E14.5, Meckel's cartilage has lengthened dramatically and straightened into an arrowhead shape, with both cartilage arms convex relative to each other. The distal cartilage tip now points rostrally upward, and ossification has progressed. At E15.5, the jaw has increased in size in proportion with the rest of the head, and ossification has progressed further. (Scale bar, 400 μm.)

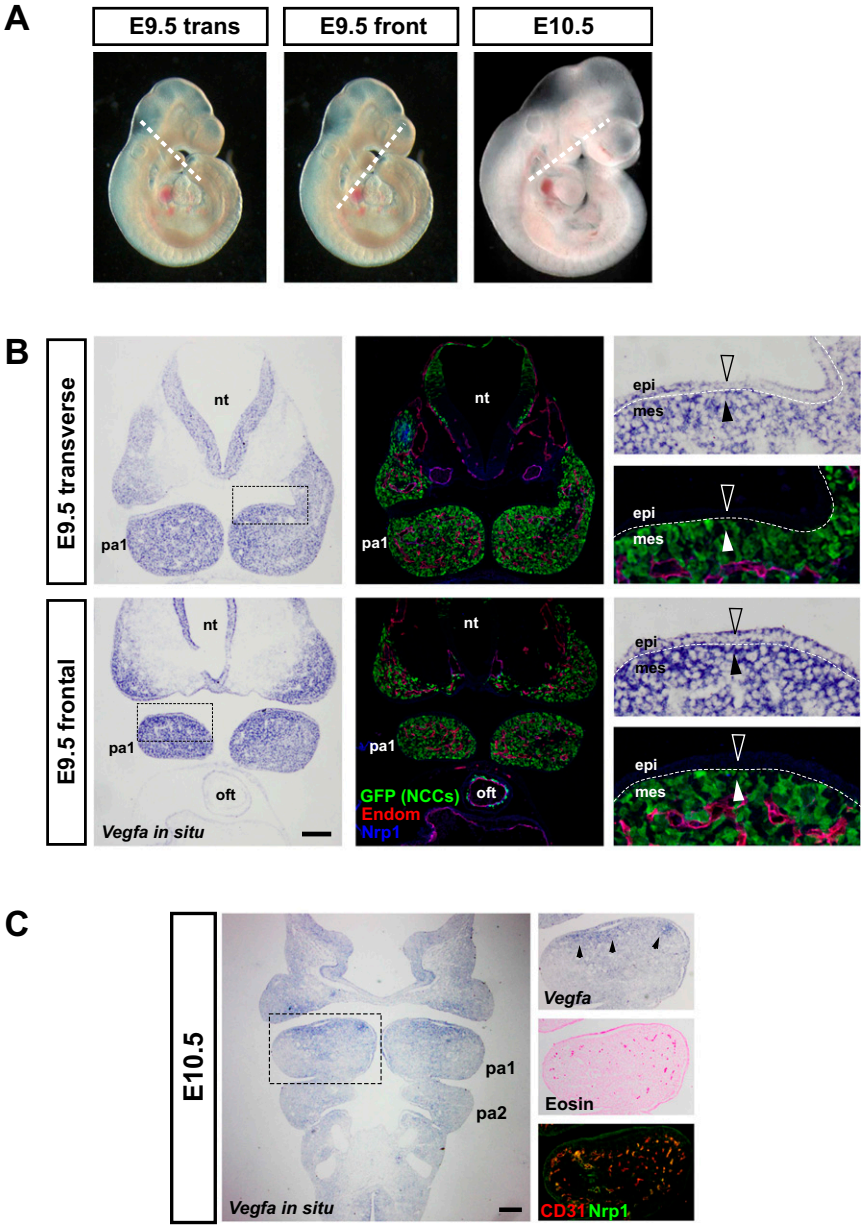

Fig. S4. Expression of *Vegfa* and colocalization with NCCs in the first pharyngeal arch at E9.5 and E10.5. (*A*) The plane of section for which the images in *B* and *C* are shown is indicated with the dashed line. (*B*) In situ hybridization for *Vegfa*. Transverse (*Upper*) and frontal (*Lower*) sections of *Wnt1-Cre;ZlEG* embryos through the first pharyngeal arch (pa1) at E9.5. (*Left*) Expression of *Vegfa* mRNA is shown, and an adjacent serial section (*Middle*) is immunostained with GFP (to highlight lineage traced NCCs), endomucin and NRP1. *Vegfa* is highly enriched in expression in NCCs migrating into and populating pa1, as shown by the overlapping expression of *Vegfa* and GFP (closed arrowheads). (*Inset*) Expression of *Vegfa* also in the epithelium (open arrowheads), but this is not a NCC-derived tissue (absent GFP expression). The developing vasculature in the mandibular arch is closely surrounded by NCC-derived mesenchyme. nt, neural tube; pa1, pharyngeal arch 1; oft, outflow tract of heart; epi, epithelium; mes, mesenchyme. (Scale bar, 100 μm.) (*C*) At E10.5, *Vegfa* expression is maintained in pa1 and expressed broadly, but enriched in the anterior domain of the mandibular arch, pa1 (arrowheads). Immunostaining of a serial section for CD31 and NRP1 indicates a dense network of vessels and the forming nerve bundle. (Scale bar, 100 μm.)

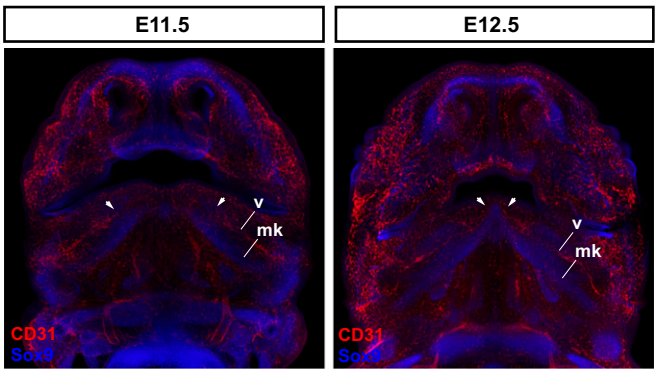

Fig. S5. Association of blood vessels and cartilage during jaw development. Whole-mount jaws from wild-type E11.5 and E12.5 embryos were immunostained with Sox9 to mark Meckel's cartilage (mk) and CD31 to mark vessels (v). At E11.5, the precursor of Meckel's cartilage is evident but has not yet fused at the distal tip. The primitive mandibular artery is present running lateral and parallel to Meckel's cartilage and extends distally to the extent of Meckel's cartilage (arrowheads). At E12.5, the two arms of Meckel's cartilage have fused at the tip, and concomitantly the mandibular vessel has extended to the tip of the cartilage (arrowheads).

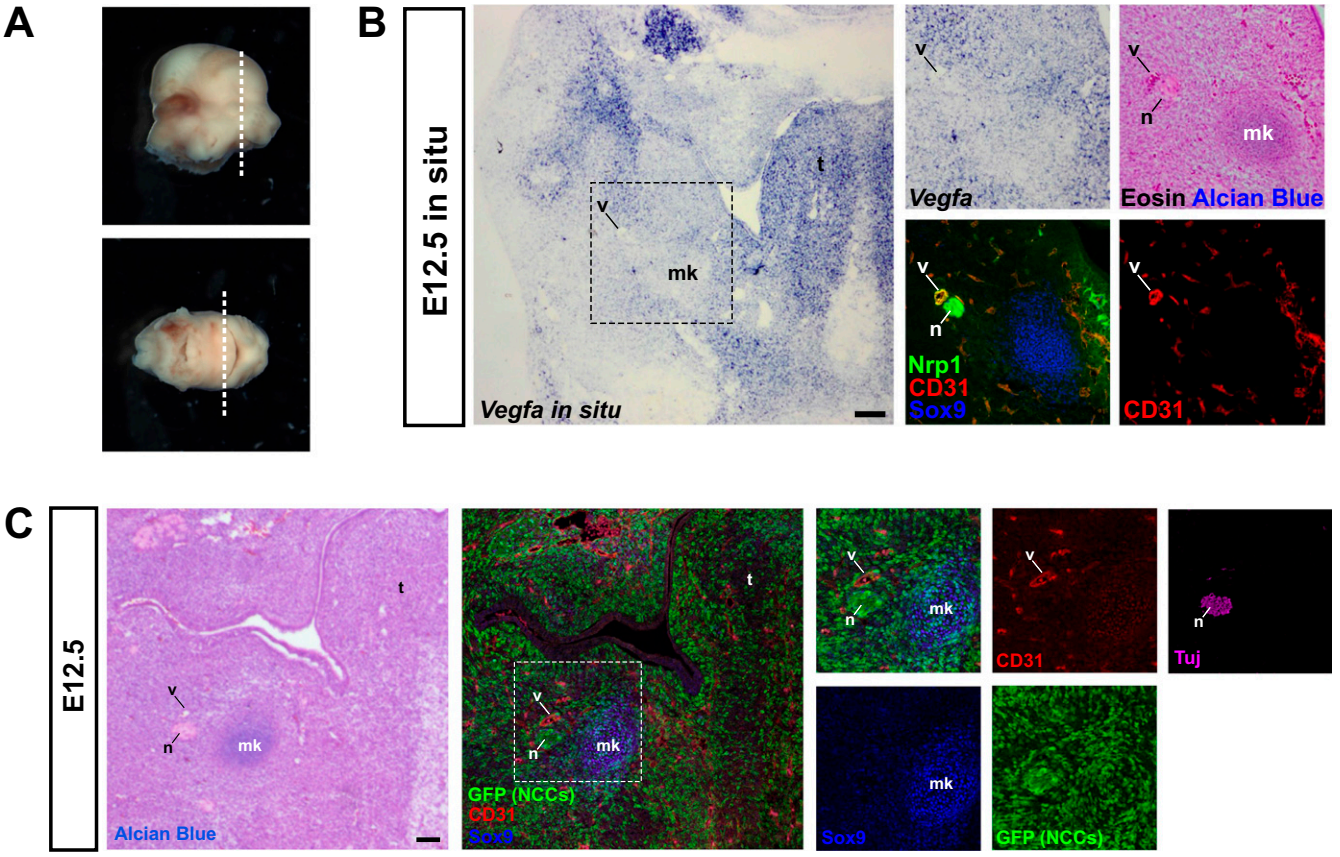

Fig. S6. Expression of *Vegfa* and colocalization with NCC-derived tissues in the mandible at E12.5. (*A*) The plane of section for which the images in *B* and *C* are shown is indicated with the dashed line. (*B*) In situ hybridization for *Vegfa*. Frontal section through the face of a wild-type E12.5 embryo, showing a medial plane of the developing mandible. At E12.5, *Vegfa* mRNA is expressed widely in the jaw, including in the mesenchyme surrounding the mandibular vessel (v) and in Meckel's cartilage (mk). Immunostaining of a serial section for CD31, NRP1, and SOX9 indicates the position of the vessel, nerve, and Meckel's cartilage, respectively. (Scale bar, 100 μm.) (*C*) Frontal sections through a *Wnt1-Cre;ZlEG* E12.5 embryo to highlight NCC-derived structures. (*Left*) A section stained with Alcian blue highlights the condensing Meckel's cartilage (mk). A neurovascular bundle containing the mandibular nerve (n) and mandibular artery (v) lies laterally adjacent to Meckel's cartilage. t, tongue. (*Middle*) A serial section immunostained for GFP, CD31 (vessels), and SOX9 (cartilage). (*Right*) Inset images of boxed area highlighted in middle panel. NCCs contribute to Meckel's cartilage and the nerve bundle and closely surround the developing mandibular vessel. A serial section is stained with the axon marker Tuj to indicate the nerve bundle. (Scale bar, 100 μm.)

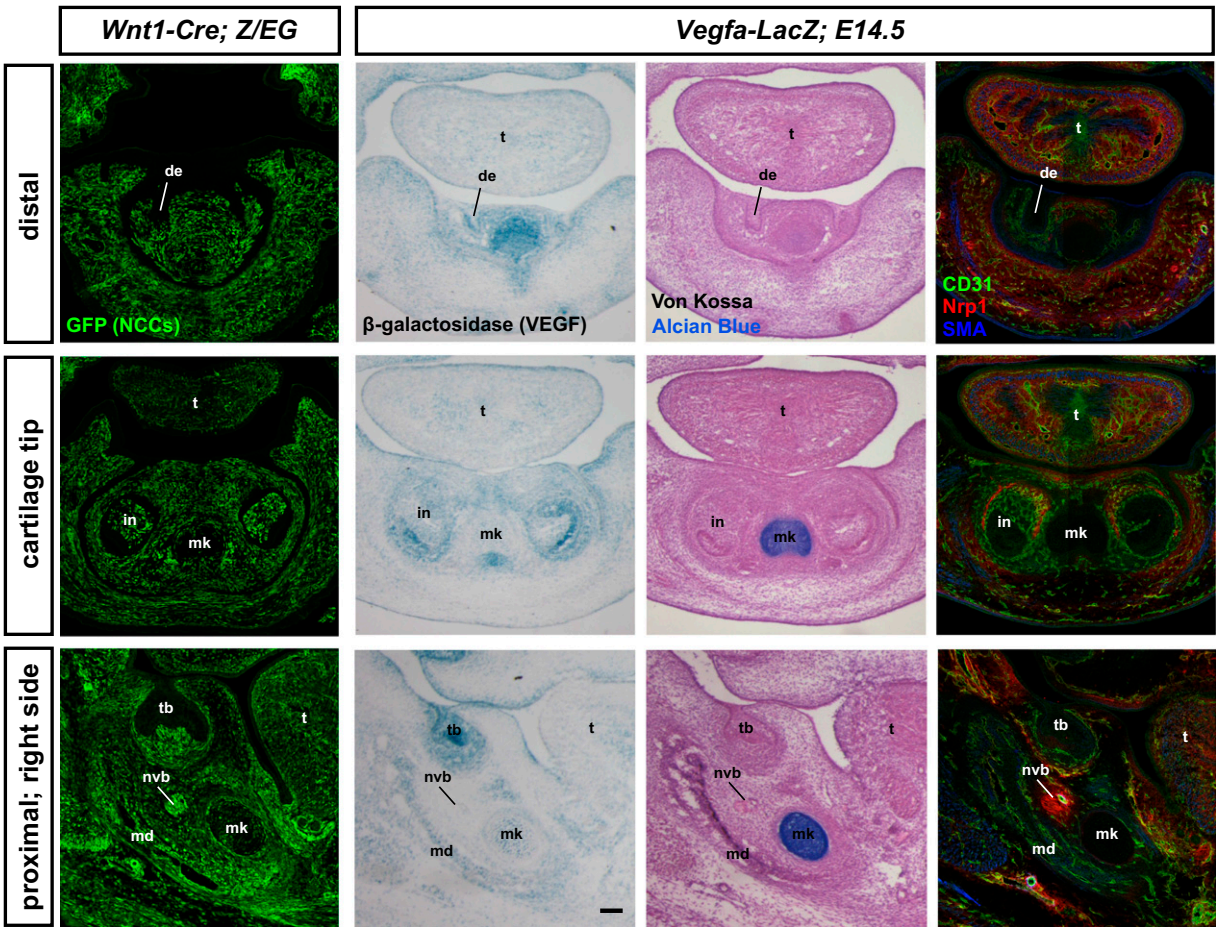

Fig. S7. *Vegfa* expression at E14.5 in *Vegfa-LacZ* embryos. (*Left*) Frontal sections through the mandible of E14.5 *Wnt1-Cre;Z/EG* embryos, with NCC-derived tissue labeled by expression of GFP. Sections were taken although the distal tip (*Upper*) of the jaw just preceding Meckel's cartilage, through the cartilage tip (*Middle*) and through the mandible proximal to the face (*Lower*). (*Right*) Serial frontal sections through the mandible of E14.5 *Vegfa-LacZ* transgenic embryos at a corresponding area to that shown for *Wnt1-Cre;Z/EG* embryos. (*Left)* Panels were stained with X-gal to reveal expression of β-galactosidase, which marks areas of *Vegfa* expression. (*Middle*) Panels were stained with Von Kossa and Alcian blue to label bone and cartilage, respectively. (*Right*) Panels were immunostained with CD31, Nrp1, and SMA. *Vegfa* is highly expressed in the region surrounding the Meckel's cartilage tip, which is also densely vascularized. *Vegfa* is also highly expressed in the teeth, although this high expression is not in the NCC-derived portion of the tooth (compare GFP-negative areas with *Vegfa* expression in the tooth bud and incisors). de, dental epithelium; t, tongue; in, incisor; mk, Meckel's cartilage; tb, tooth bud; md, mandible; nvb, neurovascular bundle. (Scale bar, 100 μm.)

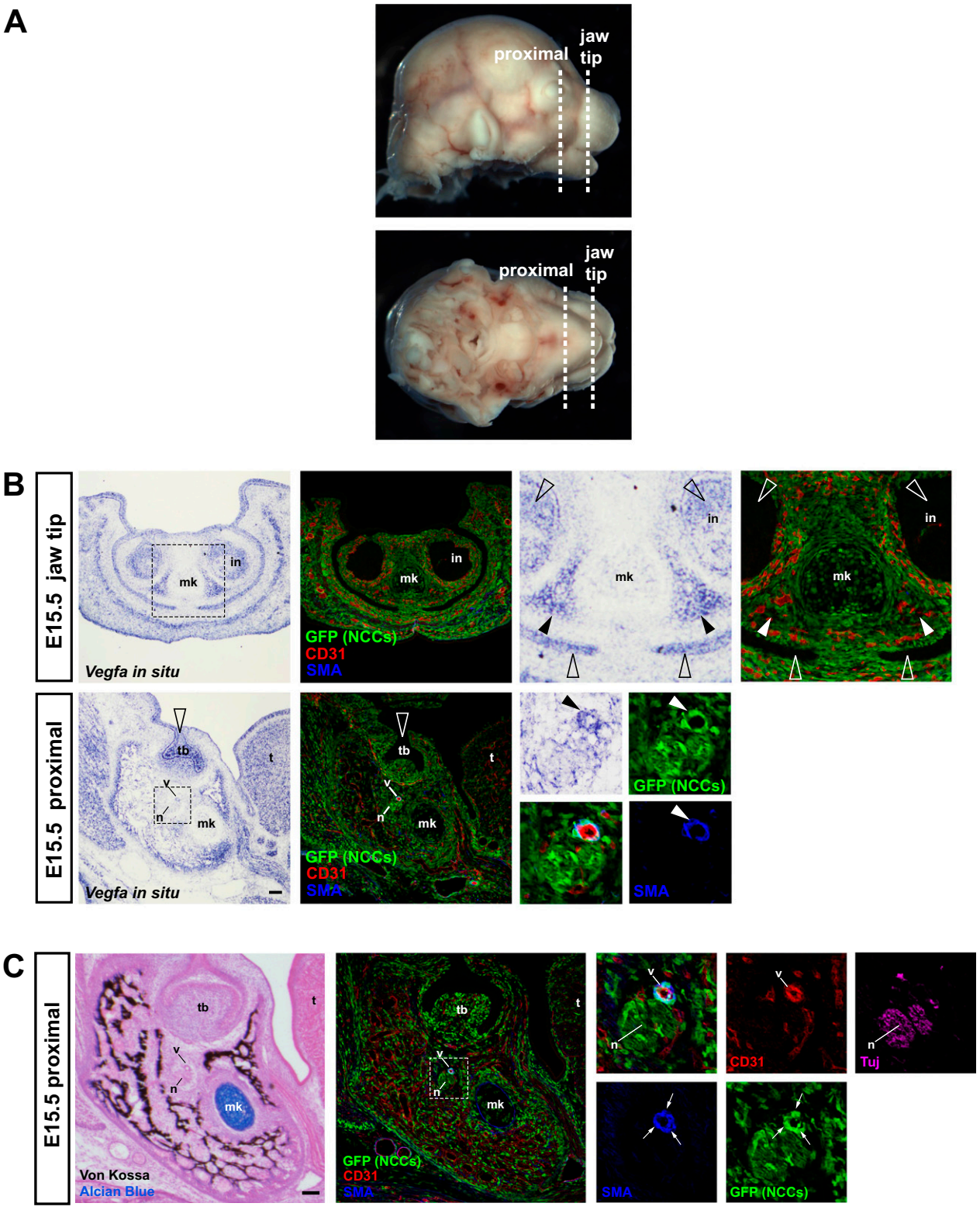

Fig. S8. Expression of *Vegfa* and colocalization with NCC-derived tissues in the mandible at E15.5. (*A*) The plane of section for which the images in *B* and *C* are shown is indicated with the dashed line. (*B*) In situ hybridization for *Vegfa*. Frontal sections through a *Wnt1-Cre;ZlEG* E15.5 embryo to highlight NCC-derived structures. (*Top*) Distal tip of Meckel's cartilage (mk), which is surrounded by tissue that highly expresses *Vegfa* (closed arrowheads). This *Vegfa* expression overlaps with GFP expression, as shown in the adjacent serial section, indicating this tissue is NCC-derived. *Vegfa* is expressed in other non-NCC-derived domains including the incisors (in) and epithelial layers (open arrowheads). (*Bottom*) Proximal serial sections through the mandible. *Vegfa* is highly expressed in the tooth bud (tb) (open arrowhead), which is non-NCC-derived, and broadly throughout mesenchymal and muscle tissue, which is mostly NCC-derived and expresses GFP. (*Inset*) Heightened expression of *Vegfa* specifically in smooth cells of the mandibular artery (closed arrowheads), which are of NCC origin (both GFP and SMA positive). n, nerve; v, vessel; t, tongue. (Scale bar, 100 μm.) (*C*) Frontal section through mandible at E15.5. (*Left*) Section stained with Alcian blue

Legend continued on following page

and Von Kossa indicates Meckel's cartilage and the mandible ossification center, respectively. The neurovascular bundle courses lateral and parallel with Meckel's cartilage. Ossification occurs such that the developing mandible surrounds and envelops the neurovascular bundle. tb, tooth bud. (*Middle*) Serial section immunostained for GFP, CD31, and alpha-SMA identifies NCC-derived smooth muscle coating of the mandibular artery. (*Inset*) Smooth muscle coating of the mandibular artery is almost exclusively NCC-derived (arrows). (Scale bar, 100 μm.)

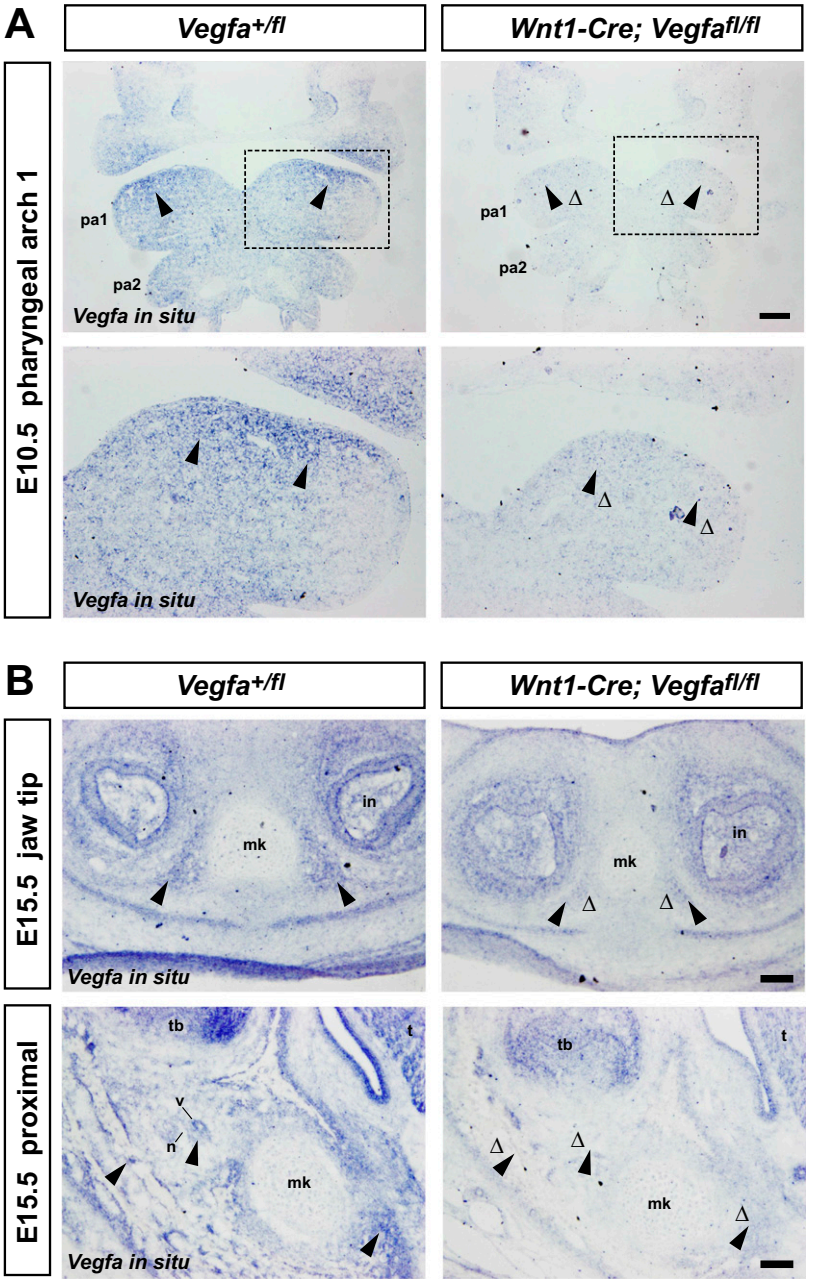

Fig. S9. Expression of *Vegfa* in *Wnt1-Cre;Vegfa*$^{fl/fl}$ *mutant embryos*. (*A*) Frontal sections through pharyngeal arch 1 (pa1) of control (*Left*) and *Wnt1-Cre; Vegfa*$^{fl/fl}$ mutant embryos (*Right*). In situ hybridization for *Vegfa* shows areas of reduced *Vegfa* expression in mutants, indicated by the Δ symbol, particularly in the neural crest-derived mesenchyme of pa1. (Scale bar, 100 μm.) (*B*) Frontal sections through the distal tip (*Top*) and proximal jaw (*Bottom*) of control (*Left*) and *Wnt1-Cre;Vegfa*$^{fl/fl}$ mutant embryos (*Right*). In situ hybridization for *Vegfa* shows areas of absent or reduced *Vegfa* expression in mutants, indicated by the Δ symbol. These include the area around the distal tip and length of Meckel's cartilage (mk), the neurovascular bundle (n and v), and in the ossifying mandible bone. These are all tissues derived from the neural crest. *Vegfa* remains expressed in non-NCC-derived tissues in the mutant such as the incisors (in), tooth bud (tb), and epithelial layers. (Scale bar, 100 μm.)

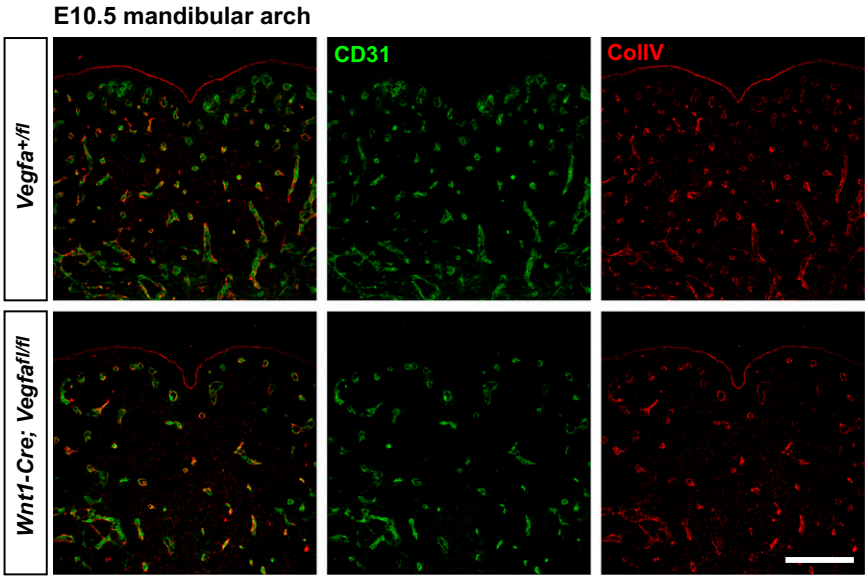

Fig. S10. Deficient angiogenesis, not vessel regression, underlies reduced vascular density in pharyngeal arch 1 at E10.5 in *Wnt1-Cre;Vegfa*$^{fl/fl}$ embryos. Frontal sections through pa1 in E10.5 control (*Upper*) and mutant (*Lower*) embryos immunostained with CD31 to label endothelial cells and collagen IV to label vessel basement membranes. Vascular density was reduced in mutant embryos. All collagen IV-positive sleeves were found to contain CD31-positive endothelial cells in both control and mutant embryos, indicating no evidence of vessel regression at this stage of development. Therefore, reduced vascular density in pa1 in *Wnt1-Cre;Vegfa*$^{fl/fl}$ mutants at E10.5 is likely a result of deficient initial angiogenesis.

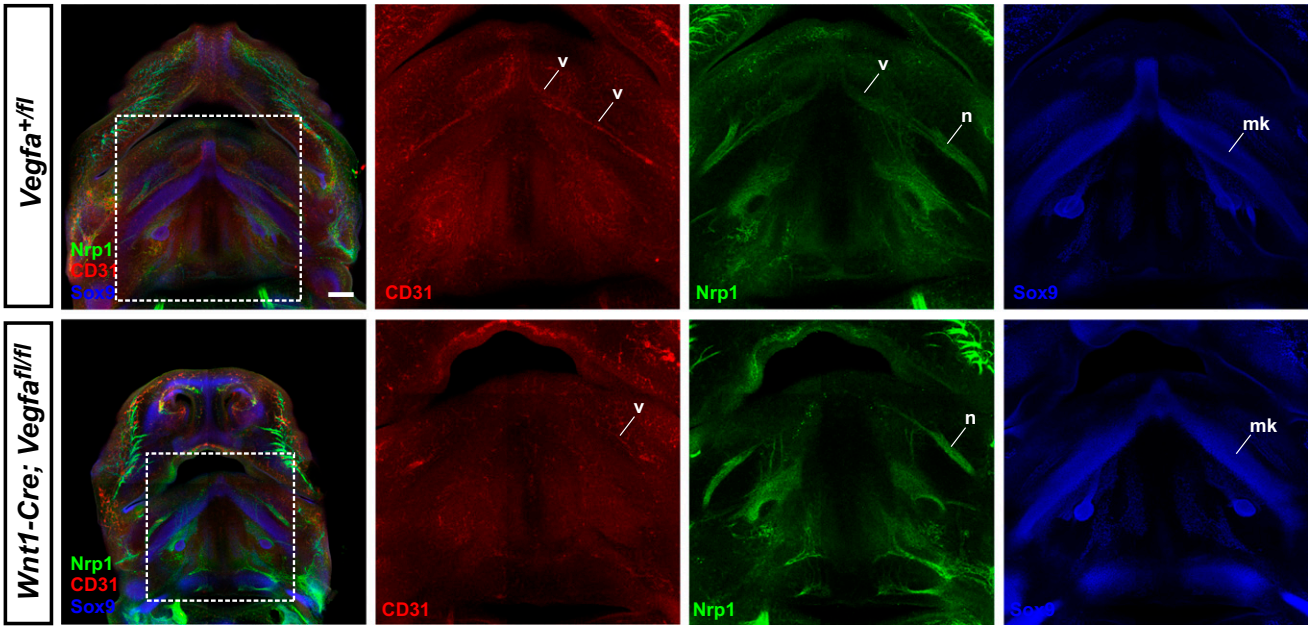

Fig. S11. Vessel defects in E12.5 *Wnt1-Cre;Vegfa*$^{fl/fl}$ mutant embryos. Whole-mount immunostaining of E12.5 jaws from control (*Top*) and mutant (*Bottom*) embryos with Sox9, CD31, and Nrp1. Specification of Meckel's cartilage appears normal in mutant embryos as Sox9 staining is indistinguishable from controls. The nerve bundle (n) running parallel to Meckel's cartilage also appears normal (Nrp1). The mandibular artery (v) appears almost absent in mutant embryos (CD31). (Scale bar, 200 μm.)

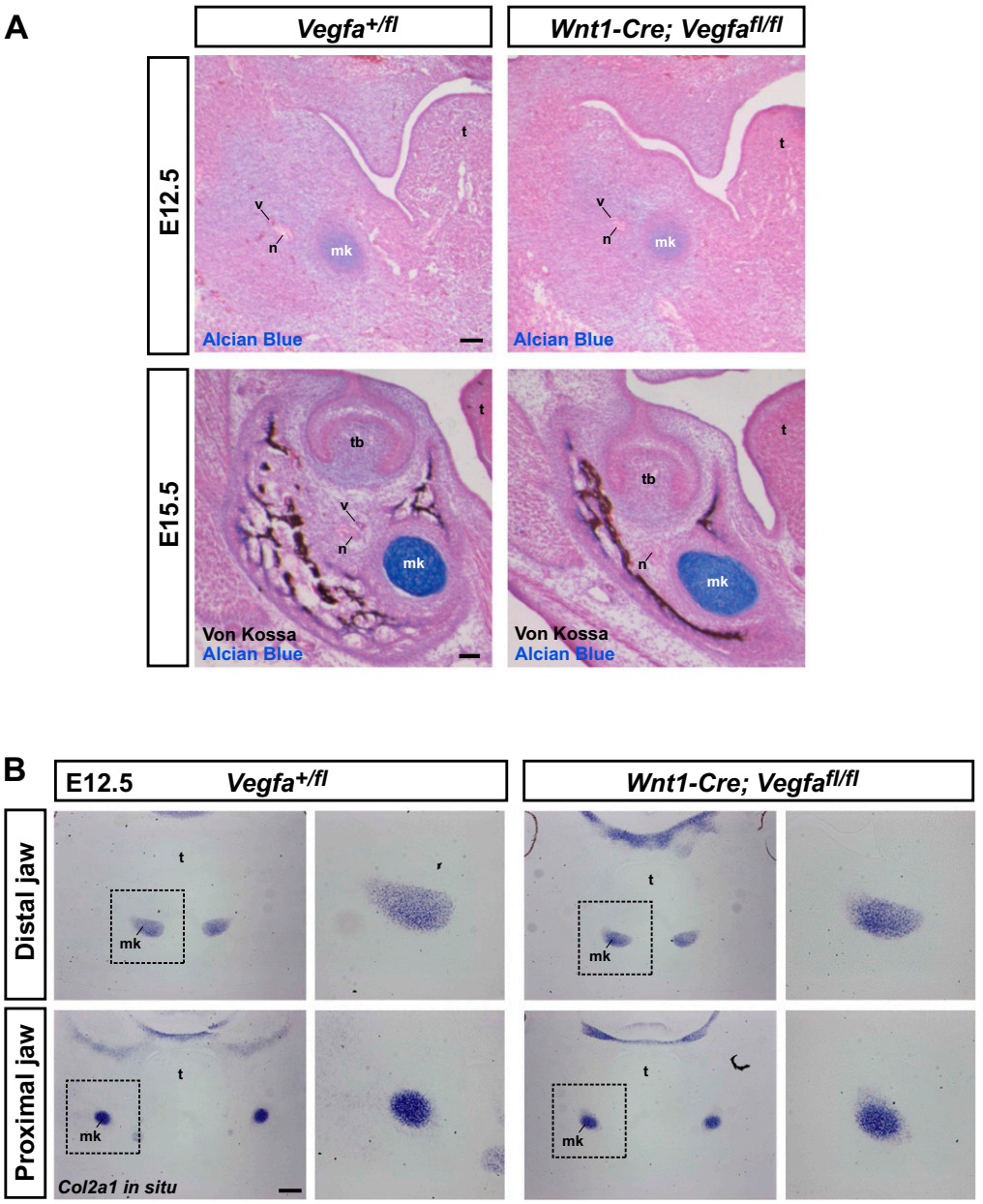

Fig. S12. Histology of *Wnt1-Cre;Vegfa*$^{fl/fl}$ jaws. (*A*, *Upper*) Frontal sections through the mandible of E12.5 control (*Left*) and mutant (*Right*) embryos. Sections were stained with Alcian blue and counterstained with eosin to highlight the presence of Meckel's cartilage and the neurovascular bundle in mutant embryos. n, nerve; v, vessel; mk, Meckel's cartilage; t, tongue. (*Lower*) Frontal sections through the mandible of E15.5 control (*Left*) and mutant (*Right*) embryos. Sections were stained with Alcian blue and Von Kossa and counterstained with eosin to indicate that the vessel component of the neurovascular bundle is lost in mutants; tb, tooth bud. (Scale bar, 100 μm.) (*B*) Frontal sections through the mandible of E12.5 control (*Left*) and mutant (*Right*) embryos. In situ hybridization for *Col2a1* mRNA shows equivalent *Col2a1* expression in Meckel's cartilage in control and mutants, suggesting cartilage specification and differentiation is unaffected. t, tongue; mk, Meckel's cartilage. (Scale bar, 200 μm.)

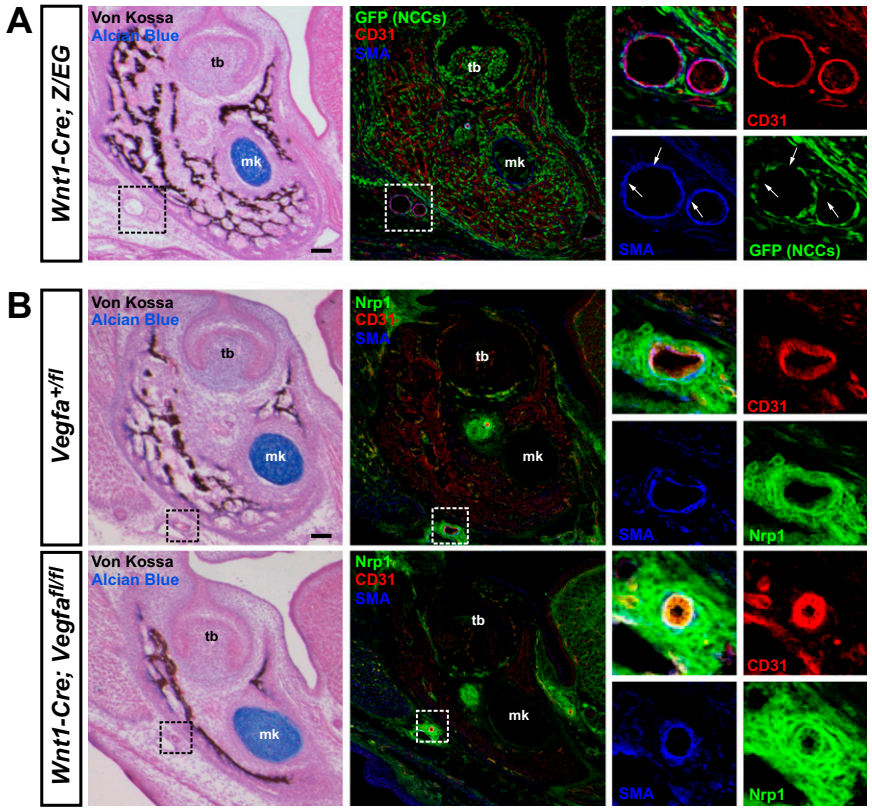

Fig. S13. Arteries with a decreased proportion of NCC-derived smooth muscle are less affected by loss of VEGF. (*A*) Frontal sections through the mandible of an E15.5 *Wnt1-Cre;Z/EG* embryo. (*Left*) Stained with Von Kossa and Alcian blue to mark bone and cartilage, respectively. (*Middle*) Serial section immunostained with CD31, SMA, and GFP to label NCC-derived tissue. Although the smooth muscle coating of the mandibular artery is almost exclusively NCC-derived (Fig. 2*C*), the smooth muscle coating of other vessels, including the facial artery (boxed; *Inset*) is of mixed mesenchymal and NCC origin and consists of many cells that are not NCC-derived (arrows). (*B*) Frontal sections although the mandible of E15.5 control (*Upper*) and *Wnt1-Cre;Vegfa*$^{fl/fl}$ (mutant; *Lower*) embryos. (*Right*) The facial artery (boxed) is highlighted. Unlike the mandibular artery, which is absent in mutant embryos (Fig. 3*D*), the facial artery is present and has a smooth muscle coating. (Scale bar, 100 μm.)

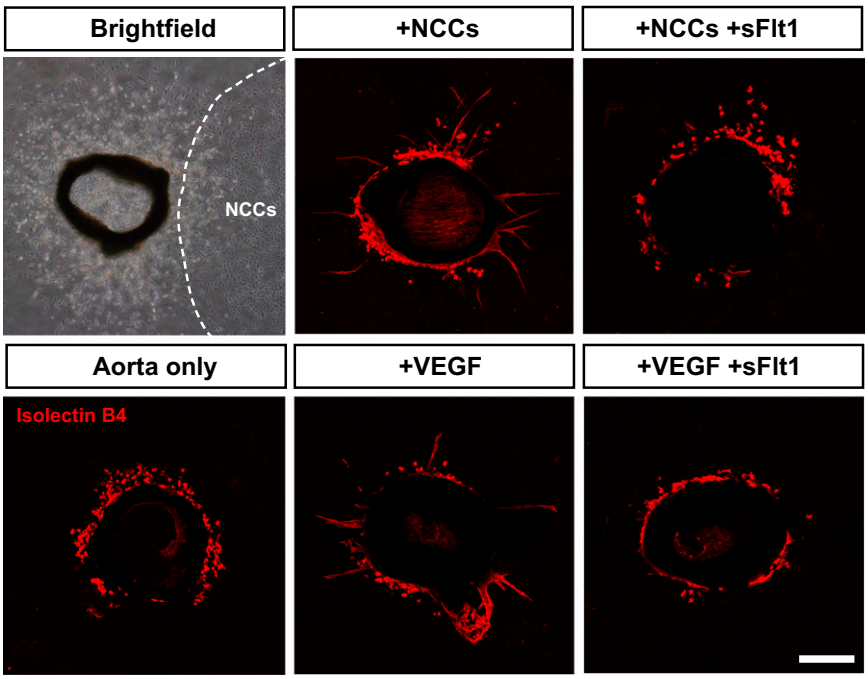

Fig. S14. NCCs induce vessel sprouting in vitro. (*Top left*) Brightfield image of aortic ring grown in a collagen matrix with primary NCC (area outlined with dashed line). Other panels: Isolectin B4 staining of aortic rings cultured with or without NCCs, or with VEGF165 and, in some experiments, with sFlt1. Coculture of aortic rings with NCCs induced vessel sprouting. Addition of sFlt-1 inhibited NCC-induced vessel sprouting. These results are presented graphically in Fig. 4*A*. (Scale bar, 200 μm.)

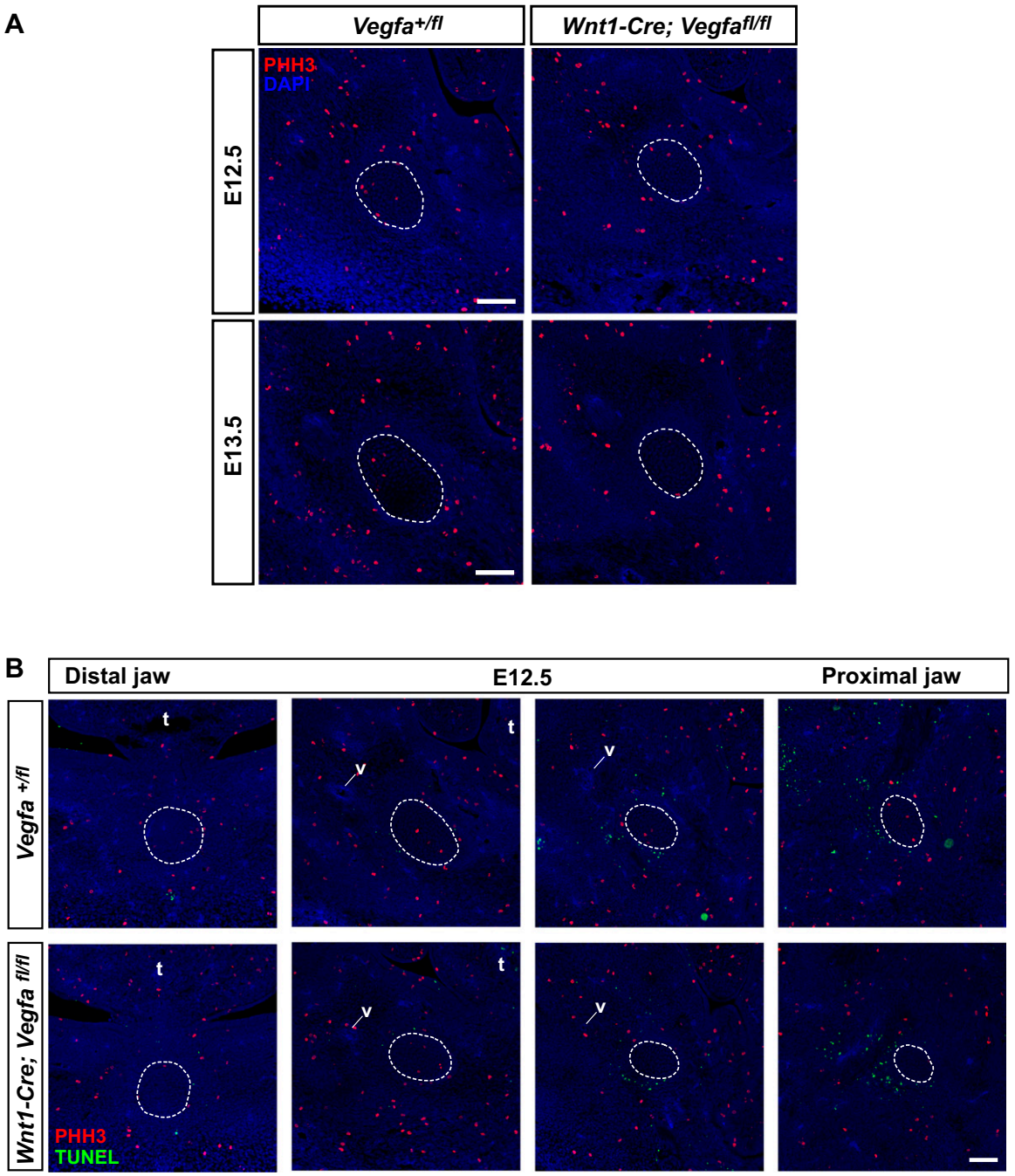

Fig. S15. Proliferation of Meckel's cartilage is reduced in *Wnt1-Cre;Vegfa*$^{fl/fl}$ embryos, with no difference in apoptosis. (*A*) Representative images of frontal sections through the mandibular region of E12.5 and E13.5 control (*Left*) and mutant (*Right*) embryos immunostained with PHH3 and DAPI. Meckel's cartilage is outlined with a dashed line. The total area inside the dashed line (in square millimeters) was measured, and the number of PHH3-positive cells was counted. These calculations are presented graphically in Fig. 3*B*. (Scale bar, 100 μm.) (*B*) Frontal sections, although the mandibular region of E12.5 control (*Top*) and mutant (*Bottom*) embryos were stained with TUNEL and PHH3. Meckel's cartilage is outlined with a dashed line. Sections at the distal jaw tip are the most left panels, and sections of the jaw proximal to the head are the most right panels. There are no gross differences in apoptosis between control and mutant embryos. t, tongue; v, mandibular blood vessel. (Scale bar, 100 μm.)

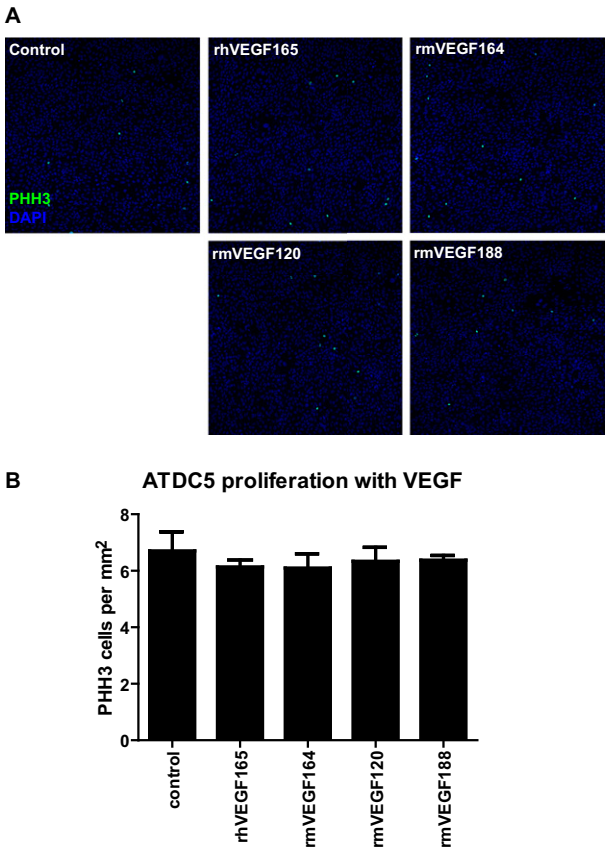

Fig. S16. Recombinant VEGF does not induce chondrocyte proliferation. (*A*) Culture of ATDC5 chondrogenic cells with addition of recombinant human VEGF165 or recombinant mouse VEGF164, VEGF120, or VEGF188. VEGF was added at 40 ng/mL, and cells cultured for 5 d, followed with staining for PHH3. The number of PHH3-positive cells per square millimeter was calculated. All recombinant VEGF proteins are from R&D Systems. (*B*) Quantitation of PHH3-positive cells per square millimeter after addition of recombinant VEGF isoforms. No isoforms of VEGF induced any change in proliferation of ATDC5 cells.

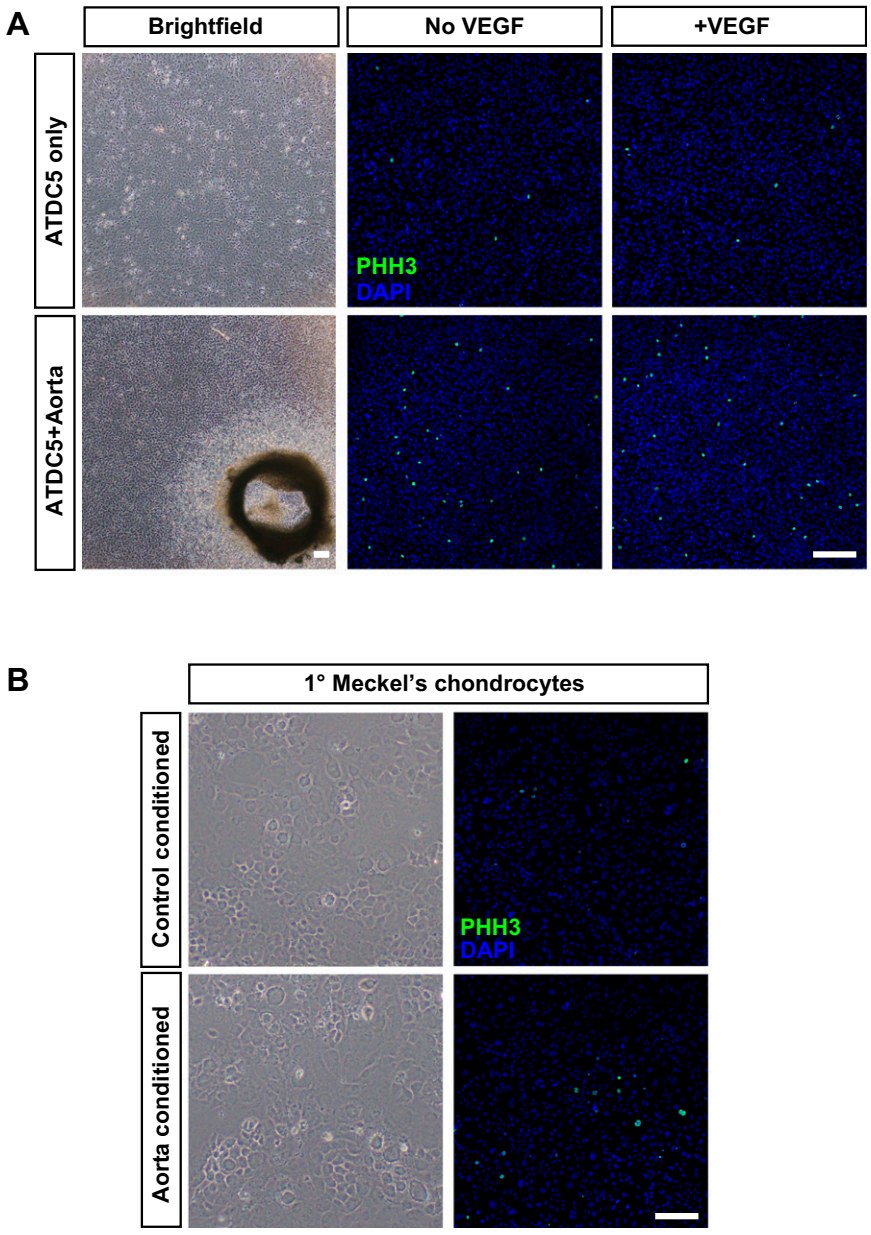

Fig. S17. Blood vessels promote chondrocyte proliferation in vitro. (*A*) Coculture of ATDC5 chondrogenic cells with aortic rings. (*Left*) Brightfield images of ATDC5 cells grown for 5 d with or without aortic rings. (*Middle* and *Right*) PHH3 staining of ATDC5 cells grown with or without aortic rings and in the presence or absence of recombinant human VEGF165. The number of PHH3-positive cells per square millimeter was calculated and presented graphically in Fig. 3*C*. (Scale bar, 200 μm.) (*B*) Culture of primary Meckel's cartilage chondrocytes, treated with control or aorta conditioned media. (*Left*) Brightfield images of primary cells grown for 5 d, showing typical chondrocytes with a refractile matrix and polygonal cobblestone morphology. (*Right*) PHH3 staining. The number of PHH3-positive cells per square millimeter was calculated and presented graphically in Fig. 3*D*. (Scale bar, 200 μm.)

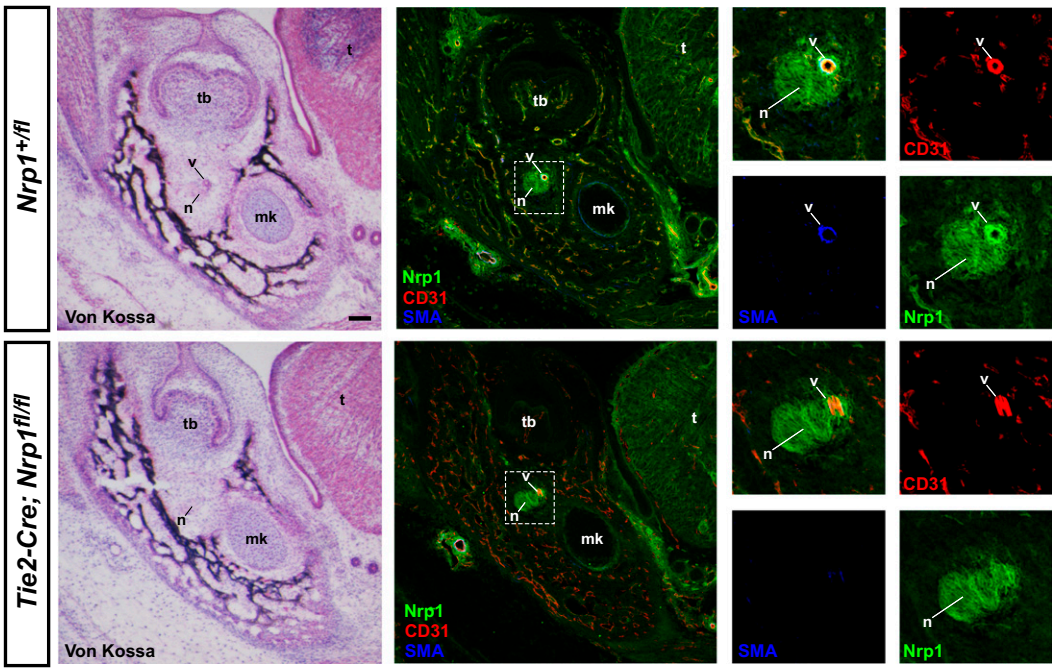

Fig. S18. *Tie2-Cre;Nrp1*$^{fl/fl}$ mutants exhibit mandibular artery defects at E15.5. Frontal sections through the mandible of E15.5 control (*Upper*) and *Tie2-Cre; Nrp1*$^{fl/fl}$ mutant (*Lower*) embryos. (*Left*) Sections stained with Von Kossa and counterstained with eosin demonstrate the mandibular vessel is severely hypoplastic in mutants. n, nerve; v, vessel; tb, tooth bud; mk, Meckel's cartilage; t, tongue. (*Middle* and *Inset*) Immunostaining of serial sections with CD31, SMA, and Nrp1. Nrp1 staining confirms expression is absent in blood vessels of mutant embryos. SMA staining reveals the mandibular vessel is not coated with smooth muscle. (Scale bar, 100 μm.)

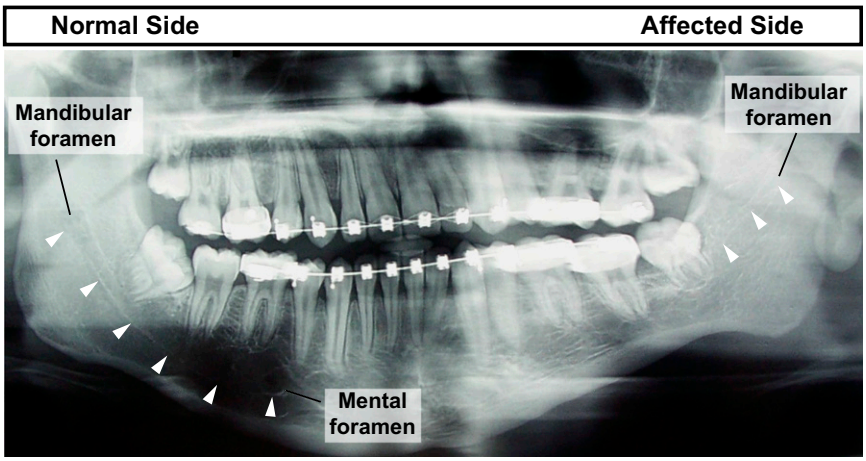

Fig. S19. Vessel defects correlate with mandibular hypoplasia in a patient with hemifacial microsomia. X-ray image of the mandible, which shows the canal of the neurovascular bundle running through the mandible (arrowheads). Although on the normal side the neurovascular bundle runs the entire length of the mandible and exits at the mental foramen, on the affected side, the bundle enters the mandible but is no longer evident past the wisdom tooth.

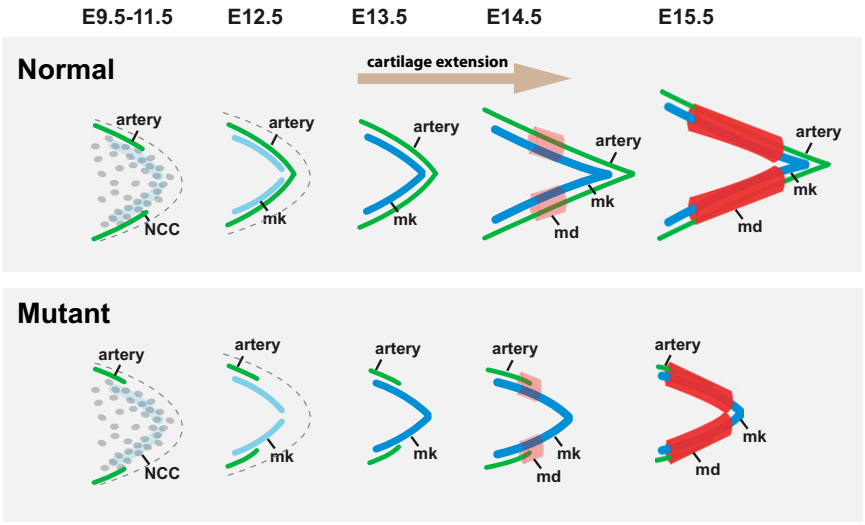

Fig. S20. A model of vessel-induced Meckel's cartilage extension to mediate jaw growth. During normal development, NCCs migrate into and populate the mandibular arch. Beginning around E11.5, NCCs condense to form the presumptive Meckel's cartilage and also surround the cartilage, giving rise to mesenchymal connective tissue and smooth muscle. The NCC-derived tissue of the mandibular arch secretes VEGF to promote vessel in-growth. By E12.5, the primitive mandibular artery runs parallel with and extends to the tip of Meckel's cartilage. At E13.5, Meckel's cartilage exhibits a typical bowed morphology, but by E14.5, the cartilage has undergone a significant extension and shape change, such that it becomes elongated and arrow-shaped. Ossification of the mandible begins at the ossification centers, and this ossification extends using Meckel's cartilage as a template to cover the entire mandible from E14.5 onward. In *Wnt1-Cre;Vegfa*$^{fl/fl}$ mutant embryos, initial NCC migration and population of the mandibular arch appear normal, as does condensation and specification of Meckel's cartilage. There is, however, a vascular defect evident as early as E9.5, and vessel density is reduced in the mandibular arch because of the lack of VEGF secretion from NCCs and the NCC-derived mesenchyme. At E12.5, the primitive mandibular artery has not formed correctly and fails to extend to the tip of Meckel's cartilage. At E14.5 and E15.5, the jaw is significantly smaller and exhibits the immature bowed morphology. Because of the lack of the mandibular artery, Meckel's cartilage has failed to proliferate and undergo the growth and shape-change transformation that typically occurs between E13.5 and E14.5. This results in a misshapen Meckel's cartilage template for the mandible to ossify around, leading to a significantly hypoplastic mandible.

Table S1. Postnatal lethality of *Wnt1-Cre;Vegfa*$^{fl/fl}$ mutants

Age	Total number of embryos/pups	Total number of mutants	Number of litters	Observed % of mutants	Expected % of mutants
Embryonic	130	37	14	28.46	25
P0–P1	23	6	4	26.09	25
P2+	24	0	4	0.00	25

Wnt1-Cre;Vegfa$^{fl/fl}$ mutants are morphologically identifiable at P0 by their craniofacial defects. When newborn, they do not appear sick. Mutants become unwell over the first 24 h and develop a reddish skin color. They display trouble breathing and lack of proper movement and do not appear to feed. Mutants appear sickly before any of the other control littermates begin to feed and have milk in their stomachs, suggesting the lethality of mutants is not a result of a lack of feeding. Mutants are born in numbers with the expected Mendelian inheritance ratio for a homozygous recessive phenotype, suggesting embryonic lethality of mutants is limited.